Weighted force analysis method for derivation of multidimensional free energy landscapes from adaptively-biased replica simulations

Fabrizio Marinelli[1]* and José D. Faraldo-Gómez [1]*

[1]Theoretical Molecular Biophysics Laboratory
National Heart, Lung and Blood Institute
National Institutes of Health, Bethesda, MD 20814

*Correspondence should be addressed to:
Fabrizio Marinelli or José D. Faraldo-Gómez
E-mail: fabrizio.marinelli@nih.gov , jose.faraldo@nih.gov

Abstract

A methodology is proposed for calculating multidimensional free-energy landscapes of molecular systems, based on post-hoc analysis of multiple molecular dynamics trajectories wherein adaptive biases are used to enhance the sampling of different collective variables. In this approach, which we refer to as Weighted Force Analysis Method (WFAM), sampling and biasing forces from all trajectories are suitably re-weighted and combined so as to obtain unbiased estimates of the mean force across collective-variable space; multidimensional free energy surfaces and minimum-energy pathways are then derived from integration of the mean forces through kinetic Monte Carlo simulations. Numerical tests for trajectories of butyramide generated with standard and concurrent metadynamics, and biased to sample one and two dihedral angles, respectively, demonstrate the correctness of the method, and show that calculated mean forces and free energies converge rapidly. Analysis of bias-exchange metadynamics simulations of dialanine, trialanine and the SH2-SH3 domain-tandem of the Abl-kinase, using up to six collective-variables, further demonstrate this approach greatly facilitates calculating accurate multidimensional free energy landscapes from different trajectories and time-dependent biases, outperforming other post-hoc unbiasing methods.

Introduction

Molecular dynamics (MD) simulations are an increasingly powerful tool to investigate complex chemical and biological mechanisms, and a means to formulate atomically detailed and physically coherent interpretations of experimental measurements[1, 2]. Too often, however, simulation studies aspire to characterize slow processes using basic algorithms, typically resulting in largely anecdotal observations and dubious mechanistic inferences. Biased-sampling techniques, by contrast, can yield quantitative information even for slow processes, provided the calculations are designed thoughtfully and analyzed rigorously. This information is ideally in the form of a landscape mapping the free energy of the molecular system as a function of one or more structural descriptors of the process of interest, formulated ad-hoc, and often referred to as collective variables (CVs)[3-5]. The minima and barriers in this landscape intuitively represent the most

probable states of the molecular system and the transition pathways that connect them, thus explaining the emergence of a mechanism [6, 7]. Among a variety of existing biased-sampling techniques, some of the most widely used are umbrella sampling (US) [8], adaptive-biasing force (ABF) [9-11] and metadynamics[6, 7, 12]. These three methods are alike in that they influence the exploration of collective-variable space by introducing biasing forces that alter the atomic trajectories; however, while in US these forces depend solely on the instantaneous molecular configuration, in Metadynamics and ABF they gradually diminish as the target space is explored, i.e. these methods are adaptive. This adaptability is arguably advantageous, although it makes rigorous derivation of free-energies more complex, from a theoretical standpoint[7, 11]. An additional difficulty is that it is non-trivial to identify *a priori* what CVs might be the most suitable for the problem at hand; it is not uncommon for intuitive descriptors to be entirely ineffective as drivers of configurational sampling. This difficulty has led to the development of specialized techniques based on reaction coordinates optimization[13-17] or enhanced biasing protocols that allow using different possible CVs, through single [18, 19] or multiple biases[20] and simulation replicas[21, 22]. To be able to sample efficiently highly dimensional collective-variable spaces is particularly important in studies of proteins and nucleic acids, as one or two descriptors are often insufficient to adequately to characterize their complex conformational mechanisms [23, 24].

The challenge ahead is thus to formulate a unified approach to derive multidimensional free energy landscapes from an arbitrary number of MD trajectories computed with different adaptive-biasing schemes and defined for multiple CVs. In previous applications, we and others have tackled this problem using the Weighted Histogram Analysis Method (WHAM) [25]. The concept is to remove the effect of the biasing potentials by rebalancing the statistical weights assigned to each of the configurations sampled in the trajectories; the corrected unbiased sampling can be then combined to obtain the best estimate of the free energy. However, for adaptive biasing approaches such as metadynamics, the application of WHAM entails a somewhat arbitrary definition of an effective biasing potential[26, 27], which is evaluated in a different manner depending on the particular biasing scheme adopted. For example, in standard metadynamics this effective potential is considered to be the time average of the biasing potential after a certain equilibration time[7, 26, 28], while in well-tempered metadynamics, this effective potential is considered to be equal to the bias potential at the end of the simulation[7, 29, 30]. Alternative formulations of WHAM that avoid the definition of an effective bias, for multiple, long simulation trajectories, would require the iterative determination of a very large number of shift constants that must be added to the biasing potentials at each of their time-updates, thus, running the risk of significant numerical errors. For similar reasons, it has been not straightforward, so far, to apply dynamic histogram[31, 32] or transition-based reweighting analysis[33, 34] in the context of adaptive biases.

Building upon the umbrella integration method[35] and its generalizations to analyze adaptively-biased simulations[36-38], we propose an alternative general approach for the calculation of multidimensional free energy landscapes, based on the calculation of the free energy gradient or mean force. This approach, which we refer to as Weighted Force Analysis Method, requires neither

the definition of effective potentials nor the iterative evaluation of additive constants. The performance of this technique is demonstrated in reference to state-of-the-art analysis methods, across different mono- and multidimensional examples (up to six dimensions) with single trajectories or multiple exchanging replicas that apply time-dependent biasing potentials along different CVs.

Theory

Mean forces estimate from multiple time-dependent biased simulations

To introduce the formulation, we assume to have a set CVs, $\boldsymbol{\xi}^{\boldsymbol{f}}(\boldsymbol{X}) = \left(\xi_1^f(\boldsymbol{X}), \xi_2^f(\boldsymbol{X}), \dots, \xi_N^f(\boldsymbol{X})\right)$, that are functions of the molecular configurations, $\boldsymbol{X}$. Let us define the free energy as a function of those CVs as:

$$F(\boldsymbol{\xi}) = -\frac{1}{\beta} ln\rho_0(\boldsymbol{\xi}) = -\frac{1}{\beta} ln \int exp\,\{-\beta U(\boldsymbol{X})\}\delta\left(\boldsymbol{\xi} - \boldsymbol{\xi}^{\boldsymbol{f}}(\boldsymbol{X})\right) d\boldsymbol{X} + C \qquad (1)$$

where $\rho_0(\boldsymbol{\xi})$ is the unbiased probability density as a function of the CVs, $U(\boldsymbol{X})$ is the simulation energy function and C is a constant (and $\beta = k_B T$, in which k_B is the Boltzmann constant, T the temperature). The mean force is the negative of the free energy gradient:

$$f_{\xi_i}(\boldsymbol{\xi}) = -\frac{\partial F(\boldsymbol{\xi})}{\partial \xi_i} \qquad (2).$$

For conventional molecular dynamics (MD) simulations, instead of a Dirac delta, free energies are typically calculated using a kernel density estimator, $K_h\left(\boldsymbol{\xi} - \boldsymbol{\xi}^{\boldsymbol{f}}(\boldsymbol{X})\right)$, e.g. a Gaussian function or a simple binning, for evaluating $\rho_0(\boldsymbol{\xi})$. The latter density estimator will also induce a smoothing of the mean forces, whose accuracy in capturing the correct value depends on the width and shape of the kernel. Namely, integrating over degrees of freedom orthogonal to the CVs and using convolution rules the mean force can be expressed as:

$$f_{\xi_i}(\boldsymbol{\xi}) \cong -\langle\frac{\partial F(\acute{\boldsymbol{\xi}})}{\partial \acute{\xi}_i}\rangle_{\xi} = -\frac{\int \frac{\partial F(\acute{\boldsymbol{\xi}})}{\partial \acute{\xi}_i}\rho_0(\acute{\boldsymbol{\xi}})K_h(\boldsymbol{\xi} - \acute{\boldsymbol{\xi}})d\acute{\boldsymbol{\xi}}}{\int \rho_0(\acute{\boldsymbol{\xi}})K_h(\boldsymbol{\xi} - \acute{\boldsymbol{\xi}})d\acute{\boldsymbol{\xi}}} = \langle\frac{1}{\beta}\frac{\partial lnK_h(\boldsymbol{\xi} - \acute{\boldsymbol{\xi}})}{\partial \xi_i}\rangle_{\xi} \qquad (3).$$

In which the notation $\langle \dots \rangle_{\boldsymbol{\xi}}$ denotes a local average around $\boldsymbol{\xi}$. For the particular case of a Gaussian density estimator, eq. 3 becomes equivalent to the typical estimate obtained through harmonically restrained simulations[39, 40], $f_{\xi_i}(\boldsymbol{\xi}) \cong k_{\xi_i}\langle\xi_i^f(\boldsymbol{X}) - \xi_i\rangle_{\xi}$, meaning that the restraint force is counterbalanced by the mean force, where k_{ξ_i} is the force constant on ξ_i and $\langle \dots \rangle_{\boldsymbol{\xi}}$ denotes an average performed over the frames of the restrained simulation. However, for standard MD simulations, calculating mean forces through eq. 3 and integrating them (based on eq. 2), does not provide any practical advantage over evaluating directly the probability density in eq. 1. By contrast, mean forces evaluations are particularly convenient for obtaining free energies from multiple biased simulation, as we describe below.

Let us consider the case of a set of trajectories, denoted with the index r, on which a time-dependent bias potential, $V_r(\boldsymbol{\xi}, t)$, is applied, which may entail a different biasing scheme (e.g. standard or well-tempered metadynamics[7, 41]) or act on different subsets of the CVs depending on the trajectory (as in bias exchange metaynamics[21]). Additionally, as expected for properly set metadynamics[6, 7, 12] or adaptive biasing force simulations[9-11], we assume a slow time variation of $V_r(\boldsymbol{\xi}, t)$ such that the simulations can be considered constantly at equilibrium.

In the WHAM[25] based approach that we used in our previous studies[26, 27, 30, 42, 43], the unbiased probability density, $\rho_0^r(\boldsymbol{\xi})$, for trajectory r, was obtained based on umbrella sampling re-weighting[8, 25] according to an effective bias potential, $\bar{V}_r(\boldsymbol{\xi})$, namely, by adjusting the statistical weight of each simulation frame, $\acute{t}$, as:

$$\rho_0^r(\boldsymbol{\xi}) \cong \sum_{\acute{t}} exp\left\{\beta \bar{V}_r\left(\boldsymbol{\xi}\left(\boldsymbol{X}_{\acute{t}}^r\right)\right) - f_r\right\} K_h\left(\boldsymbol{\xi} - \boldsymbol{\xi}^f\left(\boldsymbol{X}_{\acute{t}}^r\right)\right) \qquad (4).$$

In which $\boldsymbol{X}_{\acute{t}}^r$ is the molecular conformation of trajectory r at time $\acute{t}$, f_r are shift constants that are iteratively evaluated and $K_h\left(\boldsymbol{\xi} - \boldsymbol{\xi}^f\left(\boldsymbol{X}_{\acute{t}}^r\right)\right)$ was typically selected as a simple binning ($K_h\left(\boldsymbol{\xi} - \boldsymbol{\xi}^f\left(\boldsymbol{X}_{\acute{t}}^r\right)\right) = 1$ if $\boldsymbol{\xi}^f\left(\boldsymbol{X}_{\acute{t}}^r\right)$ belongs to a bin centered in $\boldsymbol{\xi}$ and is zero otherwise) . The final free energies are determined by combining the unbiased probabilities from each trajectory:

$$F(\boldsymbol{\xi}) \cong -\frac{1}{\beta} ln\left(\sum_r \pi^r(\boldsymbol{\xi})\, \rho_0^r(\boldsymbol{\xi})\right) + C \qquad (5),$$

in which the terms $\pi^r(\boldsymbol{\xi})$ ensure a minimal error on the free energy (according to Poisson's statistics). Despite WHAM provides a rigorous framework for combining the sampling of multiple trajectories, owing to the time-dependent nature of the bias, there is no uniform procedure for the definition of the effective potentials, $\bar{V}_r(\boldsymbol{\xi})$, across multiple adaptive biasing schemes. For example, in standard metadynamics $\bar{V}_r(\boldsymbol{\xi}) = (t_{tot} - t_F)^{-1} \int_{t_F}^{t_{tot}} V_r(\boldsymbol{\xi}, t) dt$[7, 26, 28] while in well-tempered metadynamics $\bar{V}_r(\boldsymbol{\xi}) = V_r(\boldsymbol{\xi}, t_{tot})$[7, 29, 30, 44], where t_{tot} is the total simulation time and t_F (filling time) is an equilibration time after which the bias potential can be considered approximately stationary. A strategy to avoid resorting to effective biasing potentials would be to use directly the instantaneous bias potential, $V_r(\boldsymbol{\xi}, t)$, and apply eq. 4 for small simulation intervals,Δt, e.g. at any bias potential update. Nonetheless, this would imply a different additive constant, f_r, for each bias potential update, thus leading to a large number of additive constants that must be iteratively determined.

Hereafter, we derive an alternative general approach based on the evaluation of the mean force, that does not require the definition of an effective potential nor the iterative evaluation of additive constants. Let us apply eq. 1, through the density kernel $K_h\left(\boldsymbol{\xi} - \boldsymbol{\xi}^f(\boldsymbol{X})\right)$, on a time interval, Δt, of trajectory r, that is short enough so that the bias potential can be considered time independent but large enough that the trajectory is already equilibrated. Owing to the presence of $V_r(\boldsymbol{\xi}, t)$, this operation will generally produce a biased estimate of the free energy:

$$F_b^r(\boldsymbol{\xi}, t, \Delta t) = -\frac{1}{\beta} ln \sum_{\acute{t}=t-\Delta t/2}^{t+\Delta t/2} K_h\left(\boldsymbol{\xi} - \boldsymbol{\xi}^{\boldsymbol{f}}\left(\boldsymbol{X}_{\acute{t}}^r\right)\right)$$
$$\cong -\frac{1}{\beta} ln \int exp\ \left\{-\beta\left(U(\boldsymbol{X}) + V_r\left(\boldsymbol{\xi}^{\boldsymbol{f}}(\boldsymbol{X}), t\right)\right)\right\} K_h\left(\boldsymbol{\xi} - \boldsymbol{\xi}^{\boldsymbol{f}}(\boldsymbol{X})\right) d\boldsymbol{X} \quad (6).$$
$$+ C$$

In which the right-hand side of eq. 6 arises from the equilibrium assumption[8, 35]. To relate eq. 6 to the unbiased free energy is convenient to integrate over the degrees of freedom orthogonal to the CVs: $F_b^r(\boldsymbol{\xi}, t, \Delta t) \cong -\frac{1}{\beta} ln \int exp\ \left\{-\beta\left(F(\acute{\boldsymbol{\xi}}) + V_r(\acute{\boldsymbol{\xi}}, t)\right)\right\} K_h(\boldsymbol{\xi} - \acute{\boldsymbol{\xi}}) d\acute{\boldsymbol{\xi}}$. Taking the derivatives of latter expression (and using convolutions rules), we obtain that the unbiased mean force, $f_{\xi_i}^r(\boldsymbol{\xi^c}, t, \Delta t)$, can be recovered from biased one by simply subtracting the local average of the forces arising from the bias potential:

$$f_{\xi_i}^r(\boldsymbol{\xi}, t, \Delta t)$$
$$\cong \frac{\sum_{\acute{t}=t-\Delta t/2}^{t+\Delta t/2}\left(\frac{1}{\beta}\frac{\partial ln K_h\left(\boldsymbol{\xi} - \boldsymbol{\xi}^{\boldsymbol{f}}\left(\boldsymbol{X}_{\acute{t}}^r\right)\right)}{\partial \xi_i} + \left(\frac{\partial V_r(\acute{\boldsymbol{\xi}}, \acute{t})}{\partial \acute{\xi}_i}\right)_{\acute{\boldsymbol{\xi}}=\boldsymbol{\xi}^{\boldsymbol{f}}(\boldsymbol{X}_{\acute{t}}^r)}\right) K_h\left(\boldsymbol{\xi} - \boldsymbol{\xi}^{\boldsymbol{f}}\left(\boldsymbol{X}_{\acute{t}}^r\right)\right)}{\sum_{\acute{t}=t-\Delta t/2}^{t+\Delta t/2} K_h\left(\boldsymbol{\xi} - \boldsymbol{\xi}^{\boldsymbol{f}}\left(\boldsymbol{X}_{\acute{t}}^r\right)\right)} \quad (7)$$

A general expression of the mean force can now be obtained as the weighted average[35] of all the unbiased estimates, $f_{\xi_i}^r(\boldsymbol{\xi^c}, t, \Delta t)$, obtained for all time intervals and simulations trajectories, according to the weights, $\sum_{\acute{t}=t-\Delta t/2}^{t+\Delta t/2} K_h\left(\boldsymbol{\xi} - \boldsymbol{\xi}^{\boldsymbol{f}}\left(\boldsymbol{X}_{\acute{t}}^r\right)\right)$:

$$f_{\xi_i}(\boldsymbol{\xi}) \cong \frac{\sum_r \sum_t \left(\frac{1}{\beta}\frac{\partial ln K_h\left(\boldsymbol{\xi} - \boldsymbol{\xi}^{\boldsymbol{f}}(\boldsymbol{X}_t^r)\right)}{\partial \xi_i} + \left(\frac{\partial V_r(\acute{\boldsymbol{\xi}}, t)}{\partial \acute{\xi}_i}\right)_{\acute{\boldsymbol{\xi}}=\boldsymbol{\xi}^{\boldsymbol{f}}(\boldsymbol{X}_t^r)}\right) K_h\left(\boldsymbol{\xi} - \boldsymbol{\xi}^{\boldsymbol{f}}(\boldsymbol{X}_t^r)\right)}{\sum_r \sum_t K_h\left(\boldsymbol{\xi} - \boldsymbol{\xi}^{\boldsymbol{f}}(\boldsymbol{X}_t^r)\right)} \quad (8)$$
$$= \langle\frac{1}{\beta}\frac{\partial ln K_h\left(\boldsymbol{\xi} - \boldsymbol{\xi}^{\boldsymbol{f}}(\boldsymbol{X}_t^r)\right)}{\partial \xi_i}\rangle_{\boldsymbol{\xi}} + \langle\left(\frac{\partial V_r(\acute{\boldsymbol{\xi}}, t)}{\partial \acute{\xi}_i}\right)_{\acute{\boldsymbol{\xi}}=\boldsymbol{\xi}^{\boldsymbol{f}}(\boldsymbol{X}_t^r)}\rangle_{\boldsymbol{\xi}}$$

The general meaning of eq. 8 is that the mean force is the result of the biased force arising from the combined probability density of all simulation trajectories, corrected by subtracting the local average across all trajectories, $\langle ... \rangle_{\boldsymbol{\xi}}$, of the instantaneous forces originating from the different biasing potentials applied. Note that in contrast to WHAM (eq. 4), eq. 8 does not entail effective biasing potentials nor additive constants that must be iteratively evaluated. Hence, it provides a more general formulation valid for any type and combination of adaptively-biased simulations, provided they fulfill the quasi-equilibrium assumption. For metadynamics and adaptive biasing force approaches, equilibrium conditions are more easily fulfilled after the simulation has explored the relevant regions of the CVs space, so that the forces of the bias potential oscillate around well-defined values.

As in eq. 3, the effect of the density kernel is to produce a smoothing of the mean forces, hence, a specific selection and tuning of the latter kernel may become particularly advantageous for accurate high dimensional analysis[23]. In all the applications presented in this work, mean forces were calculated according to a simple density kernel selected as a product of Gaussians (with standard deviations $\sigma_{\xi_i} = \sqrt{k_B T / k_{\xi_i}}$), for which eq. 8 becomes:

$$f_{\xi_i}(\boldsymbol{\xi}) \cong \frac{\sum_r \sum_t w_t^r(\boldsymbol{\xi}) \left[k_{\xi_i}\left(\xi_i^f(\boldsymbol{X_t^r}) - \xi_i\right) + \left(\frac{\partial V_r(\acute{\boldsymbol{\xi}}, t)}{\partial \acute{\xi}_i}\right)_{\acute{\boldsymbol{\xi}} = \boldsymbol{\xi}^f(\boldsymbol{X_t^r})} \right]}{\sum_r \sum_t w_t^r(\boldsymbol{\xi})} \quad (9),$$

where $w_t^r(\boldsymbol{\xi}) = exp\left\{-\sum_{i=1}^{N} k_{\xi_i}\left(\xi_i^f(\boldsymbol{X_t^r}) - \xi_i\right)^2 / 2k_B T\right\}$, in which the terms k_{ξ_i} can be considered as smoothing parameters that must be selected large enough so as to capture the relevant features of the underlying free energy. Note that for a single trajectory or type of bias potential, and assuming that within a small region around $\boldsymbol{\xi}$, $\left(\partial V_r(\acute{\boldsymbol{\xi}}, t)/\partial \acute{\xi}_i\right)_{\acute{\boldsymbol{\xi}} = \boldsymbol{\xi}^f(\boldsymbol{X_t^r})} \approx \left(\partial V_r(\acute{\boldsymbol{\xi}}, t)/\partial \acute{\xi}_i\right)_{\acute{\boldsymbol{\xi}} = \boldsymbol{\xi}}$, eq. 9 becomes equivalent to the expression derived by Marinova & Salvalaglio in the context of metaydnamics simulations[45]. The latter condition results in different smoothing for contributions arising from biased probability density and bias potential, and provides a reasonable alternative for analyzing metadynamics trajectories, as in the latter the biased probability density becomes gradually uniform. An advantage of eq. 8 or 9 is that they require only the instantaneous value of the biasing force, $\left(\partial V_r(\acute{\boldsymbol{\xi}}, t)/\partial \acute{\xi}_i\right)_{\acute{\boldsymbol{\xi}} = \boldsymbol{\xi}^f(\boldsymbol{X_t^r})}$, that can be easily calculated or made directly available by current enhanced sampling simulation programs[46-50].

As the mean force given by eq. 8-9 arises from a local average, error estimates can be achieved through block averages or autocorrelation analysis[11]. Assuming the same autocorrelation time for all trajectories and time intervals, the statistical error would be proportional to $\left(\sqrt{\sum_r \sum_t K_h\left(\boldsymbol{\xi} - \boldsymbol{\xi}^f(\boldsymbol{X_t^r})\right)}\right)^{-1}$, where the sum of the weights is associated to the number of effective frames around $\boldsymbol{\xi}$.

It is worth pointing out that mean forces can be also evaluated directly as a local average, around $\boldsymbol{\xi}$, of the instantaneous forces arising from the simulation energy function, $U(\boldsymbol{X})$, and effectively projected along the CVs[9-11, 51-53]. Assuming equilibrium condition, such local average would not be affected by any bias potential that depends only on the CVs[49], hence providing an alternative strategy for evaluating mean forces in the context of multiple trajectories and biases. This notwithstanding, implementation difficulties and/or inapplicability in presence of constraints and multiple related CVs[11], has made this analysis unavailable for several types of CVs and simulation programs. Here, we use the latter mean force estimate in two simple mono and two-dimensional examples (see applications to butyramide) as a comparison with the proposed approach.

Multidimensional free energy landscapes from mean forces

After evaluating the mean forces on a dense set of CVs configurations $(\xi_1^\alpha, \xi_2^\alpha, \dots, \xi_N^\alpha)$, e.g. placed on a regular grid, the free energy can be calculated according to eq. 2 by mean forces integration[40]. To do this accurately and efficiently across multiple dimensions, we adopted a kinetic Monte Carlo (KMC) approach. The KMC simulations are based on a transition rate between neighboring bins, α and β, that satisfies the detailed balance[26]:

$$R_{\alpha\beta} = \left(\tau_{\alpha\beta}^0\right)^{-1} exp\{-\beta \Delta F_{\alpha\beta}\} \qquad (10),$$

in which the preexponential term was set as $\tau_{\alpha\beta}^0 = \sum_{i=1}^N \left(\left(\xi_i^\beta - \xi_i^\alpha\right)/\Delta\xi_i\right)^2$, where $\Delta\xi_i$ are the bin widths of the grid. The free energy difference between α and β, $\Delta F_{\alpha\beta} = F\left(\boldsymbol{\xi^\beta}\right) - F(\boldsymbol{\xi^\alpha})$, is obtained from the mean forces using finite differences:

$$\Delta F_{\alpha\beta} = -\sum_i \frac{\left(f_{\xi_i}(\boldsymbol{\xi^\alpha})w(\boldsymbol{\xi^\alpha}) + f_{\xi_i}\left(\boldsymbol{\xi^\beta}\right)w\left(\boldsymbol{\xi^\beta}\right)\right)}{w(\boldsymbol{\xi^\alpha}) + w(\boldsymbol{\xi^\beta})}\left(\xi_i^\beta - \xi_i^\alpha\right) \qquad (11),$$

where $w\left(\boldsymbol{\xi^{\alpha/\beta}}\right) = \sum_r \sum_t w_t^r\left(\boldsymbol{\xi^{\alpha/\beta}}\right)$ are the total weights of each of the two bins (see eq. 9).
Finally, free energies can be estimated as in eq. 1 using the bin probabilities calculated over a long KMC trajectory, $F(\boldsymbol{\xi^\alpha}) = -\beta^{-1} ln\left[\left(N_\alpha^{KMC}/\sum_\beta R_{\alpha\beta}\right)\left(\sum_\alpha N_\alpha^{KMC}/\sum_\beta R_{\alpha\beta}\right)^{-1}\right]$, where N_α^{KMC} is the number of times the KMC trajectory visits bin α. The KMC simulations have the advantage that automatically identify the interconnected regions of the CVs space and can be easily carried out for billions of steps and eventually at raised temperature to efficiently cross free energy barriers.

Ensemble reweighting from free energy analysis

The unbiased distribution from the sampling of all trajectories can be easily recovered considering that the biasing potentials depend only on the CVs, hence, within a small bin of the latter variables the sampling distribution remains unbiased. This implies that the statistical weight assigned to each configuration, $\Omega(\boldsymbol{X_t^r})$, in order to obtain unbiased sampling, is only a function of the CVs; $\Omega(\boldsymbol{X_t^r}) = \Omega\left(\xi_1^f(\boldsymbol{X_t^r}), \xi_2^f(\boldsymbol{X_t^r}), \dots, \xi_N^f(\boldsymbol{X_t^r})\right)$. An analytical expression for the weight can be derived by imposing that the reweighted ensemble conforms to the calculated free energy:

$$\Omega(\boldsymbol{\xi^\alpha}) = \frac{1}{N_\alpha} \exp\left\{-\frac{F(\boldsymbol{\xi^\alpha})}{k_B T}\right\} \qquad (12).$$

In which N_α is the total number of frames from all trajectories in a bin, α, of the CVs.
This reweighting scheme can be applied to the cumulative sampling of all trajectories to calculate unbiased ensemble averages or to estimate the free energy as a function of different reaction coordinates.

Minimum free energy paths calculation across multidimensional landscapes

The minimum free energy path between two configurations, α_1, α_N, of the CVs space reflects the most probable pathway observed at vanishing temperature[54]. Assuming this pathway arises from a set of stochastic transitions between bins in the CVs space, the minimum free energy path is defined by the set of transitions that maximizes the time-independent probability of a stochastic path connecting the two endpoints and evaluated at nearly zero temperature[54, 55]. The latter path probability is given by the product of the normalized pairwise transition probabilities between the associated bins, which can be derived according to the KMC rates reported in eq. 10[42, 55]:

$$P^{KMC}_{\alpha_1,\alpha_N} = P^{KMC}_{\alpha_1,\alpha_2} P^{KMC}_{\alpha_2,\alpha_3} \dots, P^{KMC}_{\alpha_{N-1},\alpha_N} \quad (13).$$

In which $P^{KMC}_{\alpha_i,\alpha_j} = R_{\alpha_i,\alpha_j} / \sum_{\alpha_j} R_{\alpha_i,\alpha_j}$ is the probability to observe a transition between α_i and α_j. In this case the rates of eq. 10, R_{α_i,α_j}, are evaluated using a very low temperature, in which we consider that the approximation of a preexponential factor evaluated by a geometric term instead of a diffusion rate[26] is sufficient to identify a most likely pathway. The minimum free energy pathways reported in this work were obtained using first a global search with KMC trajectories and then a refinement step in which new pathways are generated by randomly selecting two intermediate configurations along the current pathway and running a KMC trajectory that connects them. The sampled pathways are accepted or rejected according to a Monte Carlo (MC) scheme that samples the distribution $exp\{-log(P^{KMC}_{\alpha_1,\alpha_N})/T_{MC}\}$, in which T_{MC} represents a dimensionless temperature factor. Different MC runs are carried out by gradually reducing T_{MC} using a simulated annealing protocol in order to converge to the most probable pathway.

Computational details

Simulations of solvated butyramide and alanine dipeptide were carried out with the CHARMM22 force field[56]. Metadynamics simulations of solvated butyramide were carried out at 298 K and 1 bar with a 1-fs time step and periodic boundary conditions, using NAMD version 2.14[57] and colvars[49]. Van der Waals and short-range electrostatic interactions were cut off at 12 Å; the particle-mesh Ewald method was used to calculate long-range electrostatic interactions. The molecular system comprises butyramide in a cubic box with 1467 water molecules. The metadynamics bias potentials were constructed using Gaussian hills of height 0.025 kcal mol and widths 5° and 10° for standard and concurrent metadynamics respectively. Gaussians were added every ps.

All bias exchange metadynamics simulations[21] of alanine dipeptide and Ace-Ala_3-Nme peptide were carried out with GROMACS 4.5.5/PLUMED[46, 48, 58] at constant temperature (298) and pressure (1 bar). Electrostatic interactions were evaluated with PME using a real-space cutoff of 9 Å; the same cutoff distance was used for Lennard-Jones interactions. In these simulations the metadynamics bias potential was constructed using Gaussians of height 0.024 kcal/mol and width 5.7° that were added every 2 ps. Exchanges between replicas were attempted every 2 ps.

For alanine dipeptide the simulated system entails the latter molecule and 877 water molecules enclosed in a periodic cubic box.

For the Ace-Ala$_3$-Nme peptide system the simulations were carried out using the AMBER03 force field[59] and entail Ace-Ala$_3$-Nme placed in a periodic cubic box containing 1052 water molecules.

The computational details of the simulations of the SH3-SH2 tandem of Abl kinase are reported in a previous work[43].

Results and discussion

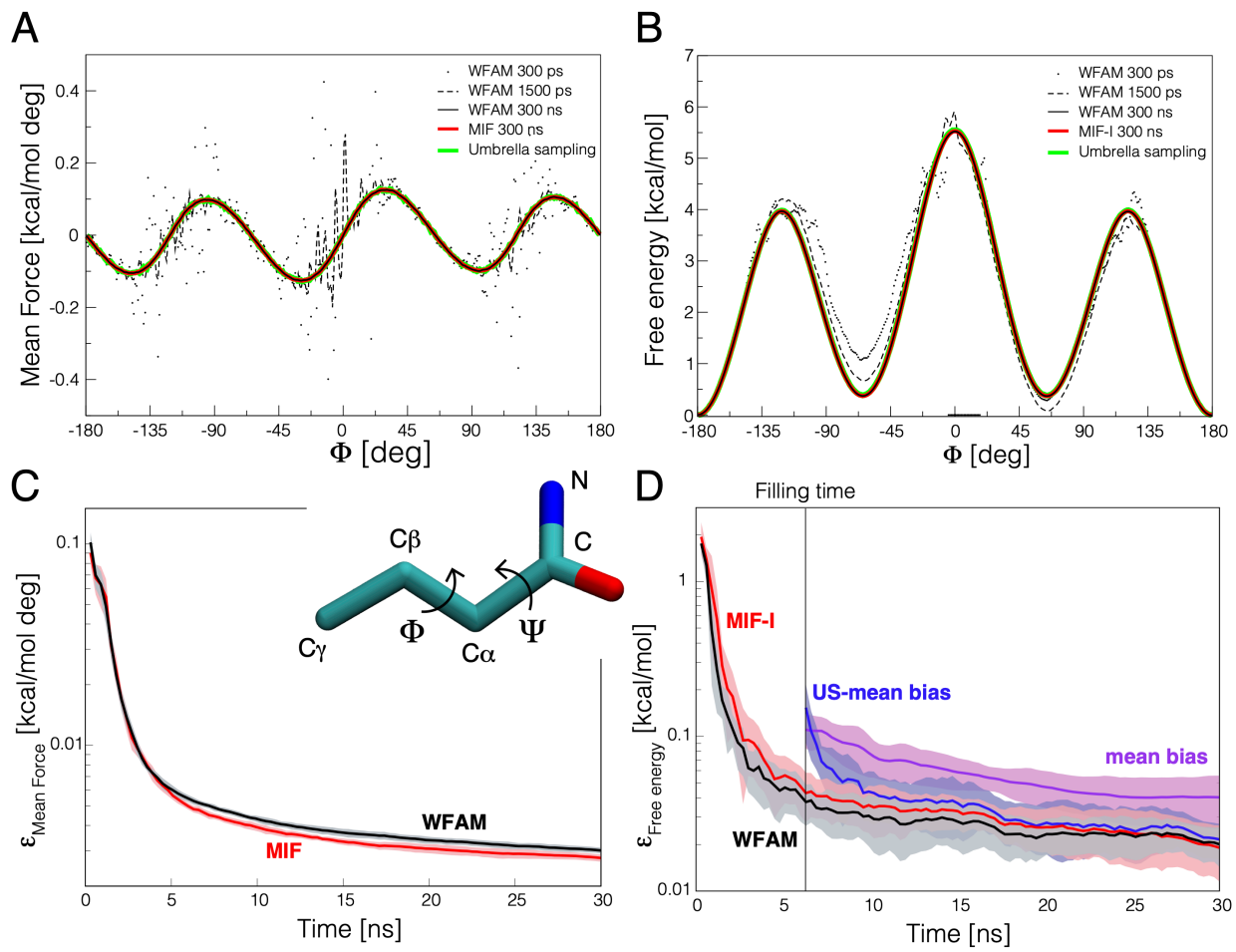

Figure 1. Benchmark test of the proposed approach on metadynamics simulations along the Φ dihedral angle of solvated butyramide. The latter molecule and its Φ and Ψ dihedral angles are illustrated in the figure. (A) Comparison between the mean forces calculated using eq. 9 (WFAM; shown for different time intervals), the mean instantaneous forces (MIF)[10] and finite differences from the free energy profile (green profile in panel B) obtained using 140 ns umbrella sampling (US) simulation[8]). (B) Comparison between the free energies obtained with 140 ns US and from numerical integration of the mean forces reported in panel A (WFAM and MIF-I; the notation -I denotes integration). (C) Time dependence of the error on the mean forces (for WFAM and MFI estimates). The error is calculated as the mean square deviation with respect to the US estimate over grid points of Φ, $\varepsilon_{Mean\ Force} = \sqrt{\sum_{i=1}^{N}\left(f(\Phi_i) - f_{US}(\Phi_i)\right)^2/N}$ (D) Time dependence of the error on the free energy for different types of free energy estimates. The error is calculated with respect to the US estimate as in $\varepsilon_{Mean\ Force}$. The purple line reflects the error

on the free energy estimated as the time average of the bias potential after the filling time[7, 26, 28].The blue line entails US corrections on the previous estimate[26]. Lines and shaded regions in panels C and D reflect average error and standard deviations over 10 independent metadynamics trajectories respectively.

Proposed approach converges with the same rate and accuracy of instantaneous forces for one-dimensional test on butyramide

To evaluate the accuracy and convergence rate of mean forces and free energies evaluated with the proposed approach, we performed a set of benchmark tests consisting of ten independent metadynamics simulations[6, 7, 12] on solvated butyramide, using the Φ dihedral angle as CV (Fig. 1). The metadynamics approach entails a time-dependent bias potential that in this case was applied on Φ and is constructed as a sum of Gaussians centered along the visited values of Φ during the trajectory. The bias potential induces on time a uniform distribution along Φ by gradually compensating the underlying free energy. Thus, after an equilibration time or filling time (~6 ns in this case, see Fig. 1D) the bias potential oscillates around the negative of the free energy profile along Φ [6, 7, 12]. For each trajectory we calculated the mean forces on grid points of Φ (spaced by 1°) using either eq. 9 or the local average of the instantaneous forces[10], which for dihedral angles can be evaluated analytically. For consistency, the latter average (evaluated as in eq. 3) was calculated using the same Gaussian density estimator adopted for estimates obtained through eq. 9 (the Gaussian standard deviation was set to 1°). The results are compared against free energy and mean forces derived from an umbrella sampling (US) simulation of 140 ns, which entails a static bias potential, $V_{US}(\Phi)$, derived from 20 ns metadynamics simulation. The free energy from US was estimated using standard histogram reweighting[8]: $F_{US}(\Phi) = -\frac{1}{\beta} ln(\rho_{US}(\Phi) exp\{V_{US}(\Phi)\})$, where $\rho_{US}(\Phi)$ is the histogram along Φ obtained from the US simulation (using a binning width of 1°). The associated mean forces were obtained by finite differences from $F_{US}(\Phi)$.

Fig. 1AB highlights how mean force and free energy profiles (obtained from mean forces integration) calculated from the combined sampling of all metadynamics trajectories (300 ns in Fig. 1AB) and estimated either with eq. 9 (WFAM in Fig. 1) or from the instantaneous forces (MIF and MIF-I in Fig. 1), perfectly match the US results. For this simple system, estimates derived from the proposed approach converge after a few ns (Fig. 1), before the metadynamics bias potential reaches a stationary condition (filling time in Fig. 1D). Reasonable values are obtained after just a few hundred ps of simulation (Fig. 1AB). Importantly, the time dependence of the error (with respect to US estimates) on mean forces and free energy (Fig. 1CD) highlight how, for this example, the proposed approach achieves the same convergence rate and accuracy of estimates obtained thorough instantaneous forces. Conversely, the free energy profile directly inferred from the time average of the metadyamics bias potential after the filling time[26, 28] (purple line in Fig. 1D) is less accurate than mean forces-based estimates. The same accuracy of latter can be instead achieved by introducing US corrections to the mean bias potential estimate[26] (blue line in Fig. 1D), which nevertheless can be evaluated only after the filling time.

Once an accurate estimate of the free energy along Φ is obtained, unbiased sampling can be recovered using the ensemble reweighting scheme provided by eq. 12. For example, this procedure can be used to calculate the unbiased histogram along the Ψ dihedral angle (Fig. 1) from the metadynamics sampling. Fig. 2 outlines the excellent accuracy of this procedure, showing that the latter histogram perfectly matches the one inferred from 400 ns MD simulation (produced for a previous work[60]).

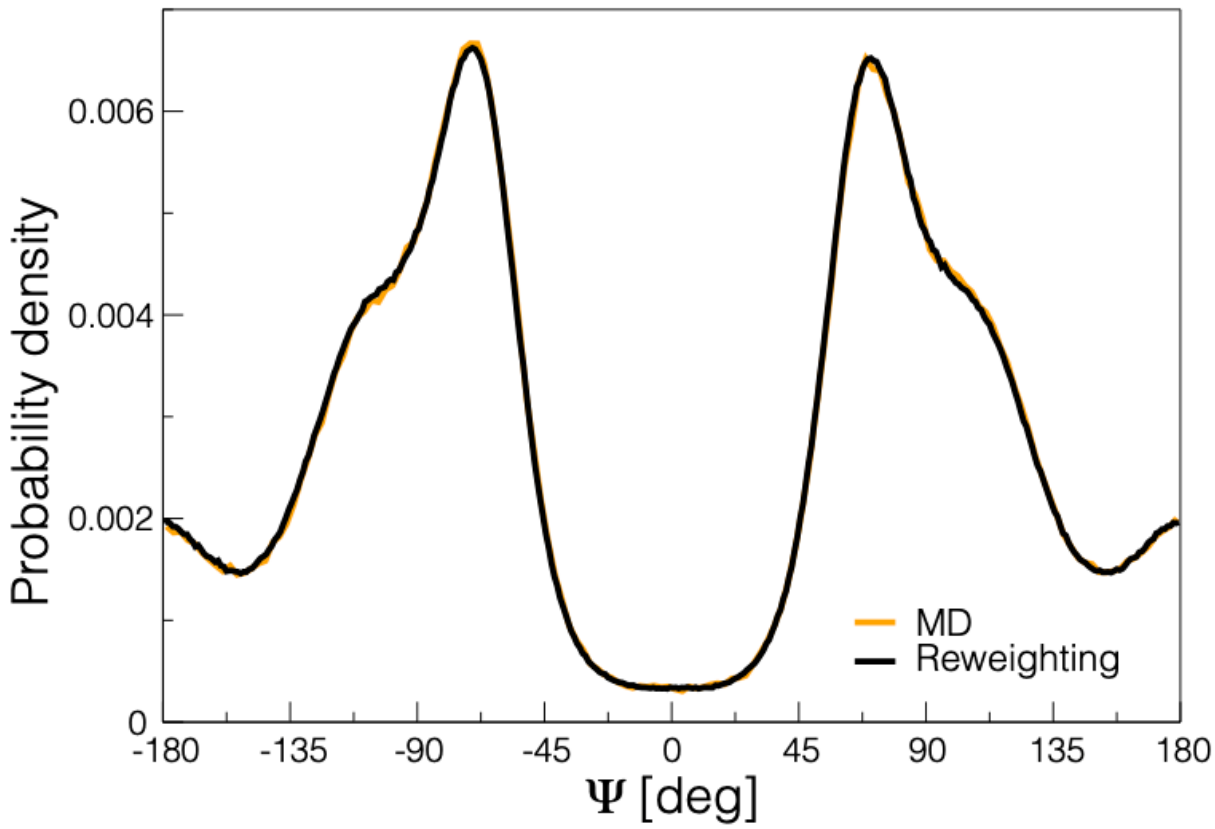

Figure 2. Unbiased probability density along the Ψ dihedral angle of butyramide obtained through 400 ns MD simulation (orange line) and ensemble reweighting using eq. 12. The reweighting was carried out on the combined sampling of 10 metadynamics simulations using the Φ dihedral angle as CV. The free energies used in eq. 12 were obtained from the integrated mean forces obtained from the metadynamics simulations using eq. 9.

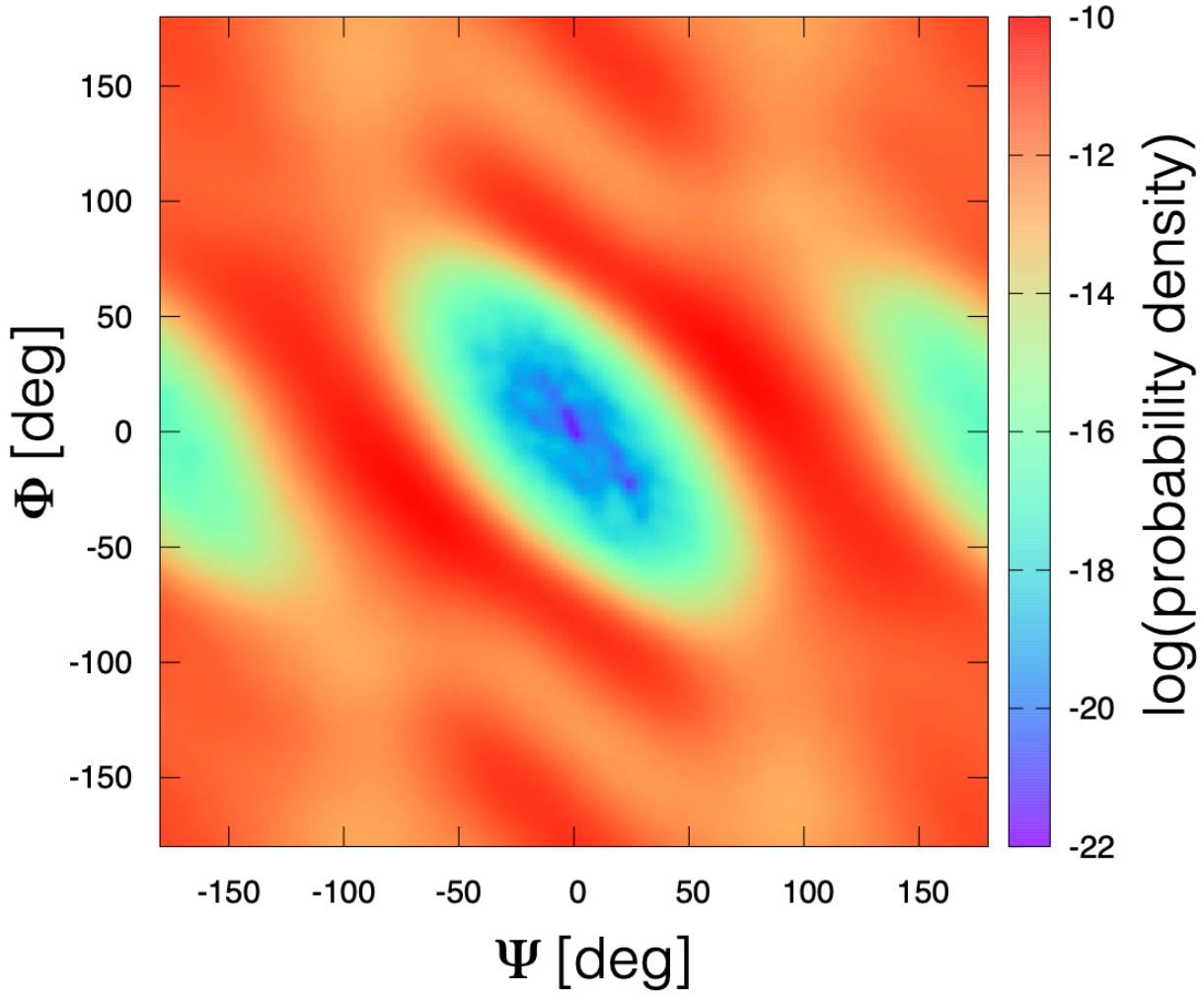

Figure 3. Logarithm of the probability density for concurrent metadynamics simulations along Φ and Ψ dihedral angles of solvated butyramide. The probability density reflects the cumulative sampling of 10 independent metadynamics simulations of 30 ns each.

Mean forces calculation provides accurate two-dimensional free energy from multiple mono dimensional biases applied to a single trajectory

To assess the ability of the proposed methodology to compute unbiased mean forces and free energy landscapes in the context of multiple mono dimensional biases applied to the same trajectory, we set out to provide a suitable analysis dataset. To do this, we generated 10 independent simulations (of 30 ns each) on solvated butyramide using concurrent metadynamics[22] on Φ and Ψ dihedral angles (Fig. 1). In these simulations, two metadynamics biasing potentials, $V_1(\Phi, t)$ and $V_2(\Psi, t)$ are applied independently on each of the dihedral angles, with an overall bias potential given by; $V(\Phi, \Psi, t) = V_1(\Phi, t) + V_2(\Psi, t)$. This type of biasing scheme produces a uniform distribution on Φ and Ψ individually, but, owing to the correlations between the two CVs, the two-dimensional space of both dihedral angles is not explored uniformly (Fig. 3). This implies that, in contrast to a standard two-dimensional metadynamics, the overall

bias potential, $V(\Phi, \Psi, t)$, does not compensate the free energy surface along Φ and Ψ, hence, it is not a free energy estimator. Similarly, the biasing potentials $V_1(\Phi, t)$ and $V_2(\Psi, t)$ do not compensate the free energy profiles along Φ and Ψ respectively. To verify whether the correct two-dimensional free energy can be recovered from mean forces calculation, we divided the space of Φ and Ψ in a regular grid of spacing 2.5° in each direction and for each grid point we calculated the mean force using eq. 9 or the mean instantaneous force[53]. The density estimator was in both cases the product of two Gaussians of standard deviation 2.5°. Free energies were obtained from mean forces integration using KMC. The accuracy of the obtained mean forces and free energy is assessed against the corresponding estimates derived from an US simulation of 110 ns. The US simulation entails a static bias potential on Φ and Ψ arising from a previous two-dimensional metadynamics simulation (of 75 ns) that explores uniformly the Φ, Ψ space. The two-dimensional free energy from US was estimated using standard histogram reweighting[8] from the US bias potential as detailed in the previous section (and using 2.5° bin spacing in Φ and Ψ). Owing to the low precision of finite differences, reference mean forces from US simulations were obtained from the local average of instantaneous forces.

In Fig. 4AB we report the force surfaces for each Φ and Ψ component and the associated free energy landscape, obtained using eq. 9 from the combined sampling of the metadynamics simulations. The force surfaces are characterized by smooth and well-defined landscapes except near the center region ($(\Phi, \Psi) \sim (0,0)$ in Fig. 4A) which is poorly sampled (Fig. 3). Owing to the integration process, the effect of noisy forces is somewhat smoothed in the associated free energy landscape. Mean forces and free energies calculated from the metadynamics simulations generally feature excellent correlation with the ones obtained from US (Fig. 4CD), regardless of the type of estimate used (either form eq. 9 or from instantaneous forces). Finally, the time dependence of forces and free energy errors (respect to US values), outlines that estimates derived with the proposed approach (WFAM in Fig. 4EF) converge with similar rate of the corresponding values calculated with instantaneous forces (MIF and MIF-I in Fig. 4EF). The mean force component along Φ calculated with eq. 9 features overall smaller error than the MIF estimate (Fig. 4E, right panel), and consequently the proposed approach provides slightly better accuracy in calculating the free energy (Fig. 4F). Such improvement in accuracy is associated to under sampled regions of the Φ, Ψ space which in this example tend to converge better using eq. 9.

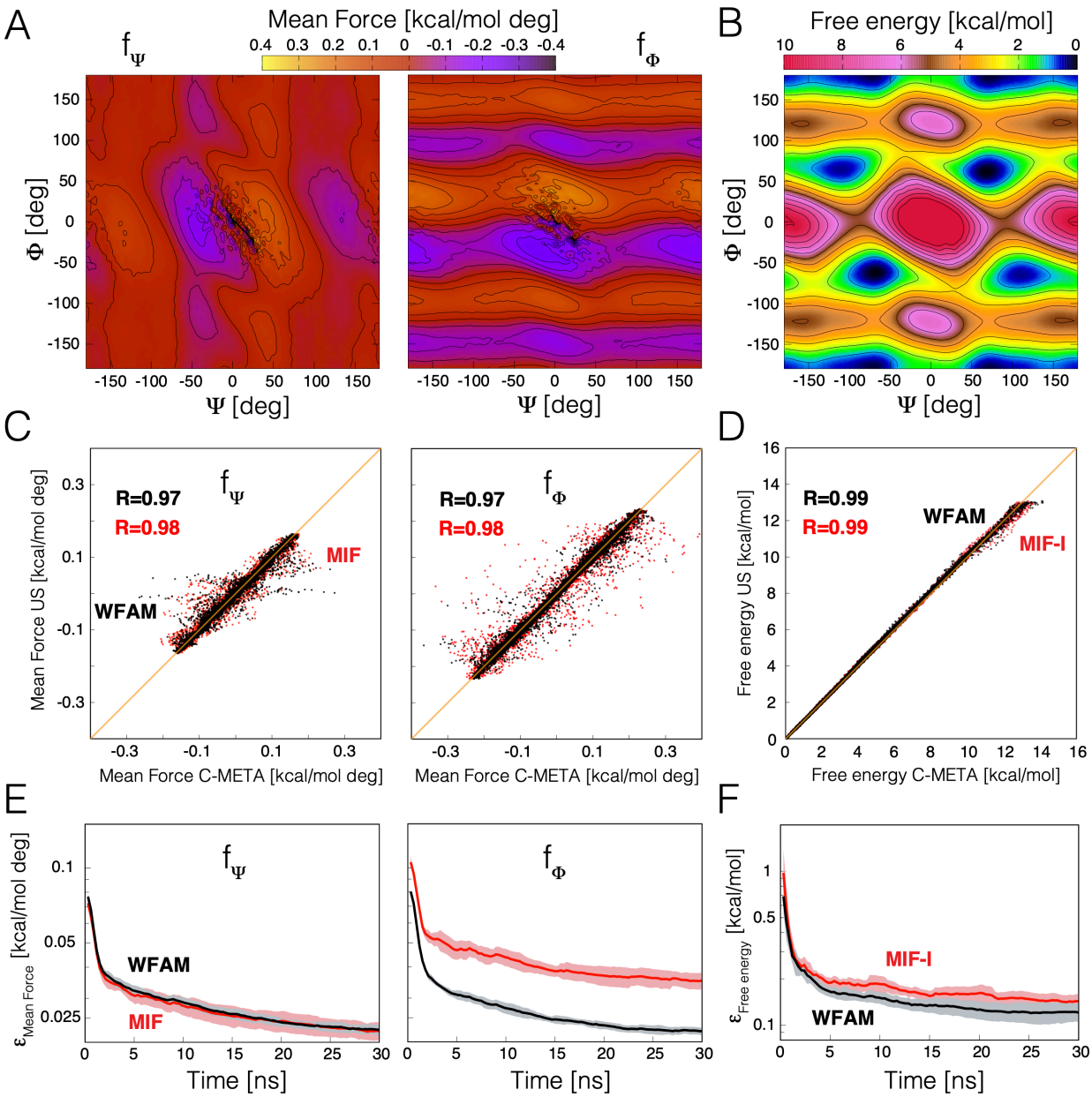

Figure 4. Assessment of convergence and accuracy of mean forces and free energy surfaces calculated with the proposed approach and mean instantaneous forces, from concurrent metadynamics (C-META) on the Φ and Ψ dihedral angles of butyramide. (A, B) Surfaces of mean forces components along Φ and Ψ (f_Φ, f_Ψ) and free energy as function of those dihedrals, obtained from 10 metadynamics simulations of 30 ns each, using eq. 9 and KMC. Contour lines are drawn every 0.05 kcal/(mol deg) and 1 kcal/mol for mean foces and free energy surfaces respectively. (C,D) Correlation plot of mean forces and free energies calculated using eq. 9 (WFAM) and mean instantaneous forces(MIF and MIF-I)[53] in reference to US estimates. (E, F) Time dependence of the error on mean forces and free energies for estimates based on eq. 9 and mean instantaneous forces. The error was calculated with respect to US estimates as explained in the caption of Fig. 1. Lines and shaded regions reflect average error and standard deviations over 10 independent metadynamics trajectories respectively

Mean forces analysis of exchanging replicas biased along different CVs provides most accurate free energy surface for alanine dipeptide

A main goal of this work is to provide a robust methodology for computing multidimensional free energy landscapes from multiple simulations with time-dependent biasing potentials applied to different CVs. Arguably one of the best examples in this regard is provided by bias exchange (BE) metadynamics simulations[21] in which many metadynamics trajectories, applying biasing potentials on different CVs are coupled together through a replica exchange scheme. Multidimensional free energies from this type of simulations are typically derived using WHAM (eq. 4 and 5)[26], which is used in this case for comparative analysis. Here, we test the capability of the proposed approach to analyze BE simulations for the solvated alanine dipeptide. For this system, we performed BE simulations using two replicas; one biased on the Φ Ramachandran torsional angle and the other on Ψ (Fig. 5). To provide a performance assessment against different biasing schemes, we carried out two independent sets of BE simulations of 400 ns each (200 ns for each replica), using either standard (META) or well-tempered metadynamics (W-META; featuring a gradual reduction of the height of the added Gaussians)[6, 7, 41]. The results are compared with the free energy obtained from ~2μs MD simulation, which was calculated according to eq. 1 from the histogram along Φ and Ψ (bin spacing of 2.5° in each direction). The two-dimensional free energy landscapes derived from MD and BE plus mean forces integration (from eq. 9 and KMC) are reported in Fig. 5A, highlighting the marked resemblance between the two maps. This figure also illustrates how, owing the presence of the biasing potentials, BE is significantly more efficient than MD in sampling high free energy regions and thus crossing free energy barriers. Nonetheless, due to the application of mono dimensional biasing potentials, BE does not achieve uniform sampling of the Φ, Ψ space. In this case, we also show an example of minimum free energy path between α_R and α_L conformations (Fig. 5A) obtained by maximizing the path probability in eq. 13. Fig. 5B outlines how, regardless of the particular metadynamics variant used to perform the simulation, there is an excellent correlation between free energies calculated with MD and BE using mean forces integration, especially at low free energies where MD is accurate. WHAM also achieves overall a very good correlation with MD (right panel of Fig. 5B), nonetheless particularly for low free energy regions features larger discrepancies (regardless of the binning used) than mean forces integration (inset of Fig. 5B). The latter deviations are also apparent from the correlation plot.

The other substantial advantage of the proposed methodology with respect to WHAM is that it provides a unified approach for the analysis of different biasing schemes. Conversely, current formulations of WHAM rely on different schemes for different metadynamics variants. For example, reweighting of standard metadynamics is based on US reweighting through the average bias potential (after filling time)[26], while in well-tempered metaydnamics the latter reweighting is carried out using the bias potential at the end of the simulation[7, 29].

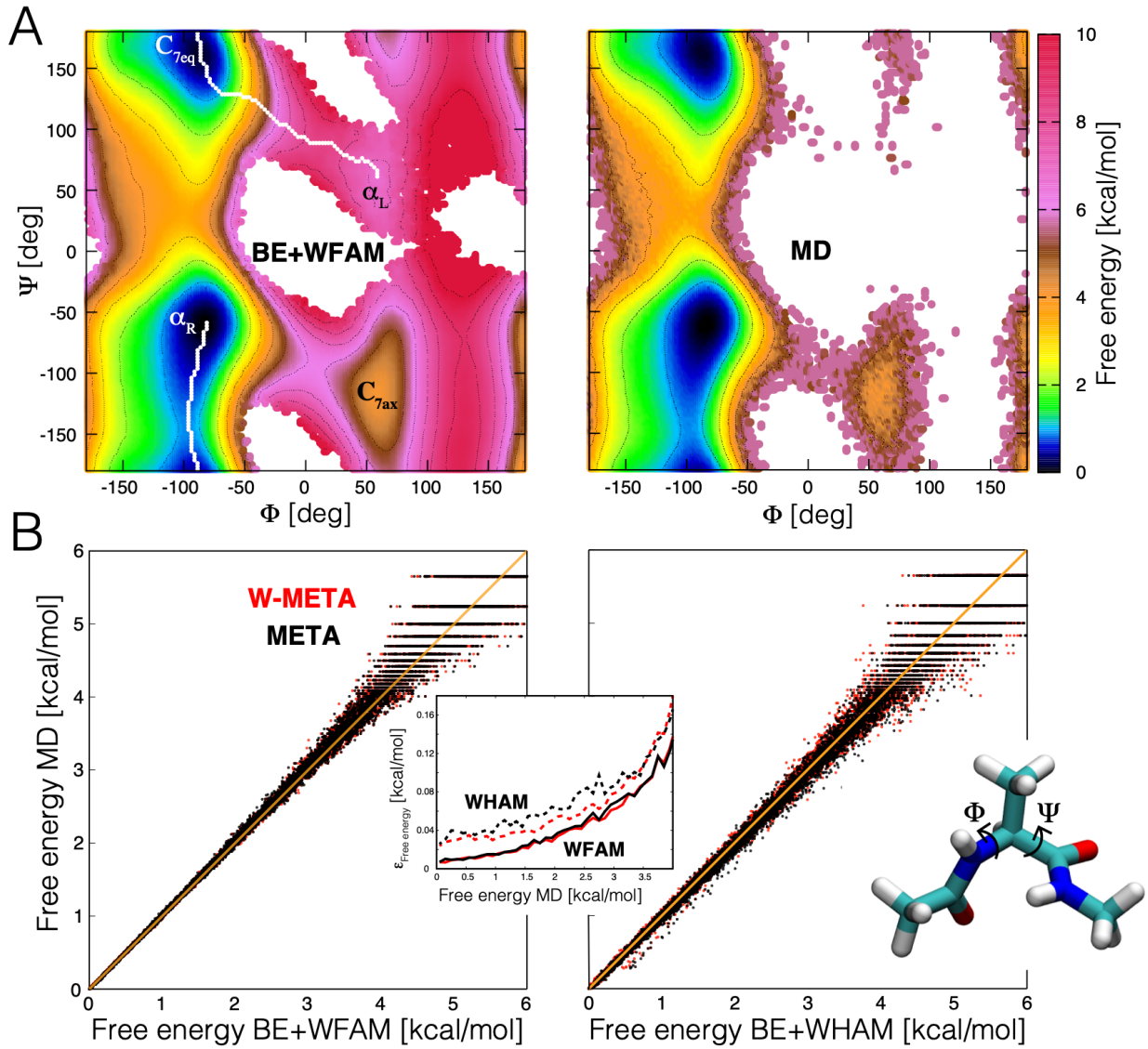

Figure 5. Comparative analysis of two-dimensional free energy landscapes of alanine dipeptide derived from MD and BE using either mean forces integration or WHAM. (A) Free energy map as a function of the Φ and Ψ dihedral angles of alanine dipeptide calculated using BE plus mean forces integration (left panel; BE simulations are performed using standard metadynamics) and MD (right panel). Contour lines are drawn with 1 kcal/mol spacings. The minimum free energy path connecting α_R and α_L conformations is shown as a white dotted line. (B) Correlation plot between MD and BE free energies, in which the latter are derived either from mean forces integration (left panel) or from WHAM (right panel). Data referred to BE simulation carried out using either conventional metadynamics (META) or the well-tempered variant (W-META) are shown as black and red circles respectively. The inset of panel B reports the absolute value of the difference between free energies calculated with MD and BE, using either mean forces (solid line) or WHAM(dashed line), as a function of the free energy from MD. Reported values correspond to a running average over intervals of 0.1 kcal/mol. Black and red lines refer to META and W-META simulations respectively.

Proposed approach can be used to derive high-dimensional free energy landscapes in model and realistic systems

In the previous sections we demonstrated that the proposed methodology provides an accurate framework to derive free energy landscapes in one and two dimensions across different biasing schemes and model systems. This notwithstanding, for realistic problems it is difficult to select a small number of CVs that allow an ideal description on the investigated process, namely that closely resemble committor probabilities between relevant free energy minima[61-63]. Unless the CVs have been specifically optimized, e.g. so that they correctly capture all the slow degrees of freedom[16], a low dimensional description might merge together distinct conformations separated by barriers and/or underestimate the free energy of the latter[6]. Provided there is sufficient statistical sampling[64], a practical strategy to alleviate these problems is to increase the number of CVs used to calculate the free energy landscape. Additionally, even using optimal CVs[13-17], a high dimensional analysis is in same case strictly required to properly characterize the system under study, as for example to describe complex protein conformational transitions[23, 24].

To assess whether the proposed mean forces analysis can be used to derive accurate free energy landscapes in multiple dimensions, we sought to apply this methodology to a suitable benchmark system, namely, the Ace-Ala_3-Nme peptide[26]. For this system we performed ~1.5μs BE metaydnamics simulations using six replicas (260 ns x 6), each biased with one of the six backbone dihedral angles shown in Fig. 6A. We then used the proposed approach (eq. 9 and KMC) to analyze these simulations by calculating the six-dimensional free energy landscape as a function of all backbone dihedral angles. For comparison, the same landscape was also evaluated from ~6 μs MD simulation. To do so, we derived the six-dimensional probability density (see eq. 1) based on the same Gaussian density estimator used for computing mean forces. Despite the high dimensionality and the fine description adopted (Gaussian standard deviation and bins side of 12°), there is an excellent correlation between the two free energies (R=0.97), especially at low free energy values where MD is accurate (Fig. 6A). The average discrepancy between the two types of estimate is 0.35 kcal/mol (see inset of Fig. 6A).

After corroborating the good performance of high-dimensional mean forces-based analysis on a model system, we illustrate its application to a realistic case. In particular, we re-analyzed previously published BE simulations on the SH3-SH2 tandem of Abl kinase[43] (Fig. 6B). The latter tandem has been shown to primarily adopt the inhibitory or "on" conformation when engaged with catalytic domain and other elements, whereas X-ray crystallography[65] and MD simulations[43] revealed that it can adopt an alternative non-inhibitory, "off", conformation when isolated. These simulations comprise 32 simulations replicas (of 200 ns each) biased with different pair combinations of five total CVs. Two of these CVs monitor the relative position of protein (S1) or interdomain connector (S2) along a line connecting on and off conformations, while a third CV (S3) measures the distance from this line (in the case of S1). The other two CVs are pseudo dihedrals describing interdomain orientations. For this system we derived the free energy landscape as a function of all five CVs using mean forces integration (eq. 9 and KMC). To visualize this landscape, we constructed its projection along S1, S3 and S3 (by integrating the probability density along the remaining CVs; Fig. 6B). Consistently with our previous analysis

[43], this landscape is consistent with the notion that the isolated tandem adopts primarily the off conformation. The derived minimum free energy pathway between on and off conformations (Fig. 6BC), confirms the presence of a barrier of ~4 kcal/mol (Fig. 6C), in agreement with the observation of spontaneous transitions between these two conformations during conventional MD simulations[43].

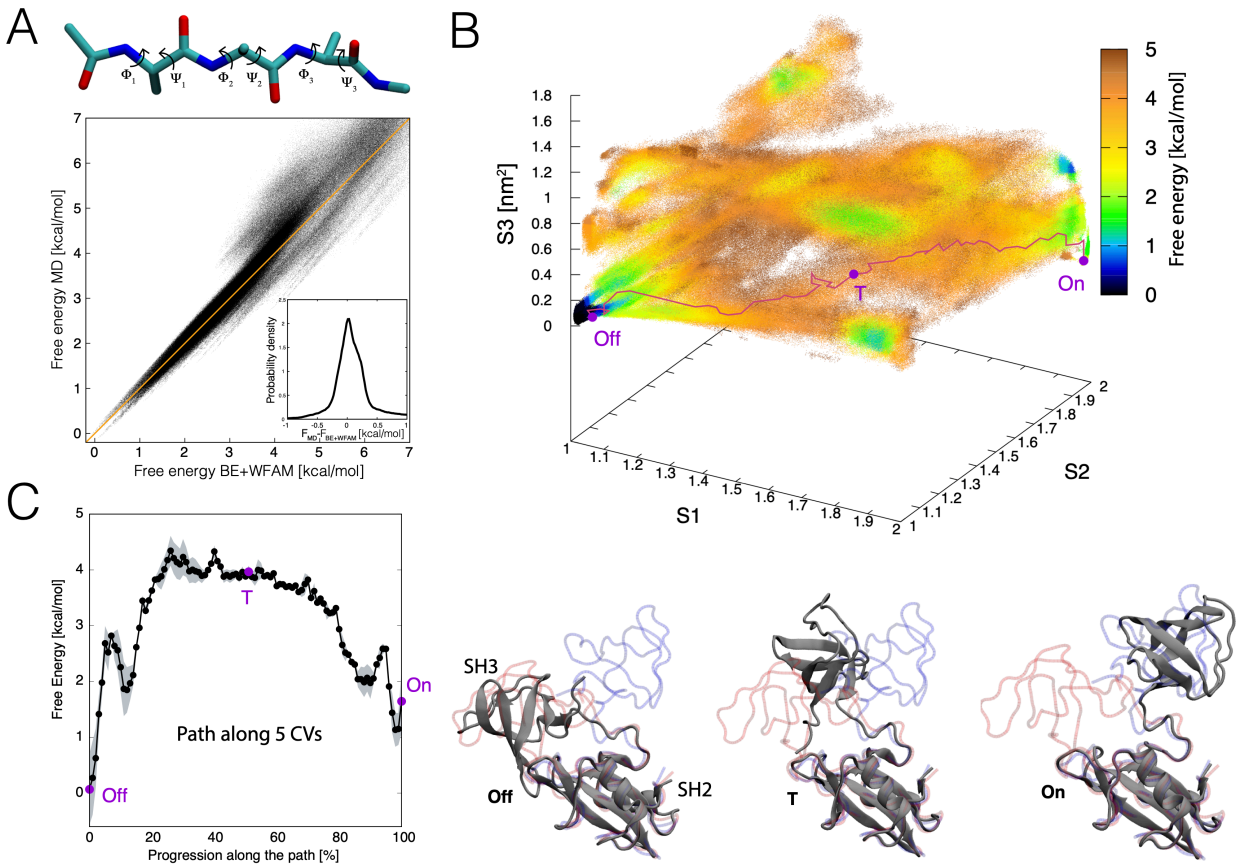

Figure 6. Application of the mean forces-based analysis to high dimensional cases. (A) Illustration of the Ace-Ala$_3$-Nme peptide and backbone dihedral angles (on panel top). Correlation plot of six-dimensional free energies obtained with standard MD and BE plus mean forces integration. Mean forces were calculated (using eq. 9) on a regular grid of 12° spacing in each direction, leading to ~2.5 millions grid points. The free energy from MD was obtained constructing the six-dimensional probability density on the same bin points using a Gaussian density estimator (same used in eq. 9). The inset reports the histogram of the deviations between free energy estimates from MD and BE plus mean forces integration. (B) Free energy landscape of SH2-SH3 tandem of Abl kinase, as a function of S1, S2 and S3 CVs (see main text). The landscape was obtained projecting the five-dimensional free energy on S1, S2 and S3. The minimum free energy pathway (see eq. 13) connecting on and off states is shown by a red line, while indicated reference configurations (purple cyrcles) are shown on the bottom of the panel in cartoon representation. The reference X-ray structures of on and off states are by the blue and red tubular representations respectively. (C) Minimum free energy pathways connecting on and off states of Abl kinase. The shaded area reflects the standard error obtained through blocks averages.

Conclusion

In this work we proposed a methodology for the accurate calculation of multidimensional free energy landscapes from multiple biased simulation. This approach builds on concepts outlined in

previous works, such as umbrella integration[35] and its variants[36-38] and is based on the calculation of the free energy gradient or mean force. Through a set of applications to model and realistic systems we demonstrated that, in contrast to previous approaches, this methodology provides a unified framework to evaluate high-dimensional free energy landscapes from different types of time-dependent biasing schemes. This comprises protocols based either on single or multiple replicas, including sets of trajectories in which biasing potentials are applied along different collective variables (CVs). The methodology relies on simple local averages to calculate the mean forces; hence, its practical application is straightforward and requires only quantities that can be easily calculated or made directly available by simulation programs. Proper application of the mean forces-based analysis requires that the simulations entail a slow time dependence of the biasing potentials and sufficient sampling such that equilibrium conditions are reasonably reached. Here we illustrated the application of the proposed approach to up six-dimensions. Practical analysis with higher dimensions can be carried out provided that there is enough sampling to perform accurate local averages in connected regions of the CVs space. A significant improvement in this regard can be provided by using specifically tuned estimators of the probability density[23]. On the systems analyzed in this work, the proposed approach showed similar accuracy and convergence rate of an alternative energetic analysis that relies on the calculation of instantaneous forces[9-11, 51-53], which, however, are not available for every type of CV and simulation setup. Furthermore, consistently with previous applications of mean forces-based approaches[35], we observed reduced statistical error compared to the weighted histogram analysis method (WHAM)[25, 26, 35]. A disadvantage compared to WHAM[26] is that the free energy can be directly derived only a as function of a set of CVs which encompasses the ones on which the biasing potentials are applied. This notwithstanding, owing to the effect of the bias potential, the sampling along those CVs is significantly improved compared to any other direction, hence, evaluated mean forces and free energies are expected to be more accurate along the latter variables. We showed that the free energy as a function of any other set of CVs or unbiased ensemble averages can be inferred from post hoc ensemble reweighting based on the free energy calculated along the initial set of CVs.

In conclusion, we have developed an effective approach to derive multidimensional free energy landscapes from different time-dependent biased trajectories. The overall methodology, including the kinetic Monte Carlo scheme used to obtain free energies from the mean forces and to calculate minimum-energy paths, are implemented in python programs which are freely available through github. Owing to the possibility of combining multiple different biased simulations and its simple applicability, we envisage that this approach will be of practical utility for calculating accurate free energies in realistic systems and help elucidate complex molecular mechanisms.

Acknowledgements

This work was funded by the Division of Intramural Research of the National Heart, Lung and Blood Institute (NHLBI), National Institutes of Health (USA) and utilized the computational resources of the NIH HPC Biowulf cluster and of the local TMB laboratory cluster.

References

1. Hollingsworth, S.A. and R.O. Dror, *Molecular Dynamics Simulation for All.* Neuron, 2018. **99**(6): p. 1129-1143.
2. Best, R.B. and K. Lindorff-Larsen, *Editorial overview: Theory and simulation: Interpreting experimental data at the molecular level.* Curr Opin Struct Biol, 2018. **49**: p. iv-v.
3. Gfeller, D., et al., *Complex network analysis of free-energy landscapes.* Proc Natl Acad Sci U S A, 2007. **104**(6): p. 1817-22.
4. Pietrucci, F., *Strategies for the exploration of free energy landscapes: Unity in diversity and challenges ahead.* Reviews in Physics, 2017. **2**: p. 32-45.
5. Chipot, C. and A. Pohorille, *Free Energy Calculations*. Springer Series in Chemical Physics. 2007: Springer-Verlag Berlin Heidelberg.
6. Laio, A. and F.L. Gervasio, *Metadynamics: a method to simulate rare events and reconstruct the free energy in biophysics, chemistry and material science.* Reports on Progress in Physics, 2008. **71**(12).
7. Bussi, G. and A. Laio, *Using metadynamics to explore complex free-energy landscapes.* Nature Reviews Physics, 2020. **2**(4): p. 200-212.
8. Torrie, G.M. and J.P. Valleau, *Non-Physical Sampling Distributions in Monte-Carlo Free-Energy Estimation - Umbrella Sampling.* Journal of Computational Physics, 1977. **23**(2): p. 187-199.
9. Darve, E. and A. Pohorille, *Calculating free energies using average force.* Journal of Chemical Physics, 2001. **115**(20): p. 9169-9183.
10. Henin, J. and C. Chipot, *Overcoming free energy barriers using unconstrained molecular dynamics simulations.* Journal of Chemical Physics, 2004. **121**(7): p. 2904-2914.
11. Comer, J., et al., *The adaptive biasing force method: everything you always wanted to know but were afraid to ask.* J Phys Chem B, 2015. **119**(3): p. 1129-51.
12. Laio, A. and M. Parrinello, *Escaping free-energy minima.* Proc Natl Acad Sci U S A, 2002. **99**(20): p. 12562-6.
13. Peters, B. and B.L. Trout, *Obtaining reaction coordinates by likelihood maximization.* Journal of Chemical Physics, 2006. **125**(5).
14. Branduardi, D., F.L. Gervasio, and M. Parrinello, *From A to B in free energy space.* J Chem Phys, 2007. **126**(5): p. 054103.
15. Diaz Leines, G. and B. Ensing, *Path finding on high-dimensional free energy landscapes.* Phys Rev Lett, 2012. **109**(2): p. 020601.
16. Tiwary, P. and B.J. Berne, *Spectral gap optimization of order parameters for sampling complex molecular systems.* Proceedings of the National Academy of Sciences of the United States of America, 2016. **113**(11): p. 2839-2844.
17. Ribeiro, J.M.L., et al., *Reweighted autoencoded variational Bayes for enhanced sampling (RAVE).* Journal of Chemical Physics, 2018. **149**(7).
18. Maragliano, L. and E. Vanden-Eijnden, *A temperature accelerated method for sampling free energy and determining reaction pathways in rare events simulations.* Chemical Physics Letters, 2006. **426**(1-3): p. 168-175.
19. Marinelli, F., *Following Easy Slope Paths on a Free Energy Landscape: The Case Study of the Trp-Cage Folding Mechanism.* Biophysical Journal, 2013. **105**(5): p. 1236-1247.

20. Pfaendtner, J. and M. Bonomi, *Efficient Sampling of High-Dimensional Free-Energy Landscapes with Parallel Bias Metadynamics.* Journal of Chemical Theory and Computation, 2015. **11**(11): p. 5062-5067.
21. Piana, S. and A. Laio, *A bias-exchange approach to protein folding.* J Phys Chem B, 2007. **111**(17): p. 4553-9.
22. Gil-Ley, A. and G. Bussi, *Enhanced Conformational Sampling Using Replica Exchange with Collective-Variable Tempering (vol 11, pg 1077, 2015).* Journal of Chemical Theory and Computation, 2015. **11**(11): p. 5554-5554.
23. Rodriguez, A., et al., *Computing the Free Energy without Collective Variables.* J Chem Theory Comput, 2018. **14**(3): p. 1206-1215.
24. Sormani, G., A. Rodriguez, and A. Laio, *Explicit Characterization of the Free-Energy Landscape of a Protein in the Space of All Its Calpha Carbons.* J Chem Theory Comput, 2020. **16**(1): p. 80-87.
25. Kumar, S., et al., *Multidimensional Free-Energy Calculations Using the Weighted Histogram Analysis Method.* Journal of Computational Chemistry, 1995. **16**(11): p. 1339-1350.
26. Marinelli, F., et al., *A kinetic model of trp-cage folding from multiple biased molecular dynamics simulations.* PLoS Comput Biol, 2009. **5**(8): p. e1000452.
27. Biarnes, X., et al., *METAGUI. A VMD interface for analyzing metadynamics and molecular dynamics simulations.* Computer Physics Communications, 2012. **183**(1): p. 203-211.
28. Crespo, Y., et al., *Metadynamics convergence law in a multidimensional system.* Physical Review E, 2010. **81**(5).
29. Branduardi, D., G. Bussi, and M. Parrinello, *Metadynamics with Adaptive Gaussians.* Journal of Chemical Theory and Computation, 2012. **8**(7): p. 2247-2254.
30. Liao, J., et al., *Mechanism of extracellular ion exchange and binding-site occlusion in a sodium/calcium exchanger.* Nat Struct Mol Biol, 2016. **23**(6): p. 590-599.
31. Rosta, E. and G. Hummer, *Free Energies from Dynamic Weighted Histogram Analysis Using Unbiased Markov State Model.* Journal of Chemical Theory and Computation, 2015. **11**(1): p. 276-285.
32. Stelzl, L.S., et al., *Dynamic Histogram Analysis To Determine Free Energies and Rates from Biased Simulations.* J Chem Theory Comput, 2017. **13**(12): p. 6328-6342.
33. Wu, H., et al., *Statistically optimal analysis of state-discretized trajectory data from multiple thermodynamic states.* Journal of Chemical Physics, 2014. **141**(21).
34. Wu, H., et al., *Multiensemble Markov models of molecular thermodynamics and kinetics.* Proceedings of the National Academy of Sciences of the United States of America, 2016. **113**(23): p. E3221-E3230.
35. Kastner, J. and W. Thiel, *Bridging the gap between thermodynamic integration and umbrella sampling provides a novel analysis method: "Umbrella integration".* J Chem Phys, 2005. **123**(14): p. 144104.
36. Zheng, L.Q. and W. Yang, *Practically Efficient and Robust Free Energy Calculations: Double-Integration Orthogonal Space Tempering.* Journal of Chemical Theory and Computation, 2012. **8**(3): p. 810-823.
37. Fu, H.H., et al., *Extended Adaptive Biasing Force Algorithm. An On-the-Fly Implementation for Accurate Free-Energy Calculations.* Journal of Chemical Theory and Computation, 2016. **12**(8): p. 3506-3513.

38. Lesage, A., et al., *Smoothed Biasing Forces Yield Unbiased Free Energies with the Extended-System Adaptive Biasing Force Method.* Journal of Physical Chemistry B, 2017. **121**(15): p. 3676-3685.
39. Vaneerden, J., et al., *Potential of Mean Force by Thermodynamic Integration - Molecular-Dynamics Simulation of Decomplexation.* Chemical Physics Letters, 1989. **164**(4): p. 370-376.
40. Maragliano, L. and E. Vanden-Eijnden, *Single-sweep methods for free energy calculations.* Journal of Chemical Physics, 2008. **128**(18).
41. Barducci, A., G. Bussi, and M. Parrinello, *Well-tempered metadynamics: A smoothly converging and tunable free-energy method.* Physical Review Letters, 2008. **100**(2).
42. Marinelli, F., et al., *Evidence for an allosteric mechanism of substrate release from membrane-transporter accessory binding proteins.* Proc Natl Acad Sci U S A, 2011. **108**(49): p. E1285-92.
43. Corbi-Verge, C., et al., *Two-state dynamics of the SH3-SH2 tandem of Abl kinase and the allosteric role of the N-cap.* Proceedings of the National Academy of Sciences of the United States of America, 2013. **110**(36): p. E3372-E3380.
44. Ono, J. and H. Nakai, *Weighted histogram analysis method for multiple short-time metadynamics simulations.* Chemical Physics Letters, 2020. **751**.
45. Marinova, V. and M. Salvalaglio, *Time-independent free energies from metadynamics via mean force integration.* J Chem Phys, 2019. **151**(16): p. 164115.
46. Bonomi, M., et al., *PLUMED: A portable plugin for free-energy calculations with molecular dynamics.* Computer Physics Communications, 2009. **180**(10): p. 1961-1972.
47. Tribello, G.A., et al., *PLUMED 2: New feathers for an old bird.* Computer Physics Communications, 2014. **185**(2): p. 604-613.
48. Bonomi, M., et al., *Promoting transparency and reproducibility in enhanced molecular simulations.* Nature Methods, 2019. **16**(8): p. 670-673.
49. Fiorin, G., M.L. Klein, and J. Henin, *Using collective variables to drive molecular dynamics simulations.* Molecular Physics, 2013. **111**(22-23): p. 3345-3362.
50. Sidky, H., et al., *SSAGES: Software Suite for Advanced General Ensemble Simulations.* Journal of Chemical Physics, 2018. **148**(4).
51. Carter, E.A., et al., *Constrained Reaction Coordinate Dynamics for the Simulation of Rare Events.* Chemical Physics Letters, 1989. **156**(5): p. 472-477.
52. Ciccotti, G., R. Kapral, and E. Vanden-Eijnden, *Blue moon sampling, vectorial reaction coordinates, and unbiased constrained dynamics.* Chemphyschem, 2005. **6**(9): p. 1809-1814.
53. Henin, J., et al., *Exploring Multidimensional Free Energy Landscapes Using Time-Dependent Biases on Collective Variables.* Journal of Chemical Theory and Computation, 2010. **6**(1): p. 35-47.
54. Maragliano, L., et al., *String method in collective variables: minimum free energy paths and isocommittor surfaces.* J Chem Phys, 2006. **125**(2): p. 24106.
55. Harland, B. and S.X. Sun, *Path ensembles and path sampling in nonequilibrium stochastic systems.* J Chem Phys, 2007. **127**(10): p. 104103.
56. MacKerell, A.D., et al., *All-atom empirical potential for molecular modeling and dynamics studies of proteins.* Journal of Physical Chemistry B, 1998. **102**(18): p. 3586-3616.

57. Phillips, J.C., et al., *Scalable molecular dynamics on CPU and GPU architectures with NAMD.* Journal of Chemical Physics, 2020. **153**(4).
58. Hess, B., et al., *GROMACS 4: Algorithms for Highly Efficient, Load-Balanced, and Scalable Molecular Simulation.* J Chem Theory Comput, 2008. **4**(3): p. 435-47.
59. Duan, Y., et al., *A point-charge force field for molecular mechanics simulations of proteins based on condensed-phase quantum mechanical calculations.* Journal of Computational Chemistry, 2003. **24**(16): p. 1999-2012.
60. Hustedt, E.J., et al., *Confidence Analysis of DEER Data and Its Structural Interpretation with Ensemble-Biased Metadynamics.* Biophys J, 2018. **115**(7): p. 1200-1216.
61. Ren, W., et al., *Transition pathways in complex systems: Application of the finite-temperature string method to the alanine dipeptide.* Journal of Chemical Physics, 2005. **123**(13).
62. Ma, A. and A.R. Dinner, *Automatic method for identifying reaction coordinates in complex systems.* Journal of Physical Chemistry B, 2005. **109**(14): p. 6769-6779.
63. Best, R.B. and G. Hummer, *Reaction coordinates and rates from transition paths.* Proceedings of the National Academy of Sciences of the United States of America, 2005. **102**(19): p. 6732-6737.
64. Scott, D.W., *Multivariate density estimation: theory, practice, and visualization*. 2015., John Hoboken, NJ, USA: Wiley & Sons.
65. Fushman, D., R. Xu, and D. Cowburn, *Direct determination of changes of interdomain orientation on ligation: Use of the orientational dependence of N-15 NMR relaxation in Abl SH(32).* Biochemistry, 1999. **38**(32): p. 10225-10230.